Aerosol Organic-Mass-to-Organic-Carbon Ratio Measurements

LYNN M. RUSSELL*

Department of Chemical Engineering, Princeton University, Princeton, New Jersey 08648

The ratio of organic-mass-to-organic-carbon, typically taken to be between 1.4 and 1.7, has an uncertainty higher than 50%, but this value is used in every measurement to date of the organic fraction of atmospheric particles. A recently developed technique with errors reduced to between 9% and 33% provides measurements of this ratio that show its large variability for samples measured in northeastern Asia and the Caribbean. The technique uses functional groups measured by FTIR spectroscopy to estimate composite organic carbon from the number of carbon bonds present and organic mass from the molecular mass of each functional group associated with the measured bond type. The molecular masses associated with each functional group are not unique and do not account for highly branched organic compositions. For the organic mixtures described by the less than 20% of atmospheric organic mass that has been speciated by GCMS, the theoretical discrepancy in the composite organic-mass-to-organic-carbon ratio is less than 5%. The measured ratios for submicron particle samples are skewed: over 90% of the measurements collected lie between 1.2 and 1.6, with mean values just below 1.4. This variability highlights the importance of measured organic-mass-to-organic-carbon ratios to reduce the uncertainty associated with atmospheric organic aerosol.

Introduction

Organic compounds are recognized as important contributors to aerosol-related consequences, including visibility, health, and climate (*1*). Aqueous-phase reactions occur in particles containing organic peroxides and other reactive compounds (*2*). Organic compounds will affect water uptake by particles, determining particle size as well as optical properties (*3, 4*). Health effects associated with the organic fraction of inhaled particles, in particular the aromatic fraction, also highlight the importance of better quantification of particulate organic matter (*5, 6*). Artifacts in organic sampling and assumptions about molecular composition have prevented quantification of the organic fraction of particle mass because systematic errors result in uncertainties as high as 50% in those measurements (*7*).

While current efforts to measure the operationally defined organic carbon mass (OC in μg C) and elemental carbon mass (EC in μg C) have increased considerably, few efforts to directly measure organic mass (OM in μg) have been undertaken (*7–11*). Organic speciation approaches require a series of time-consuming derivatization and separation techniques that identify less than 20% of OM suspended in

atmospheric particles (*12–14*). Fourier Transform Infrared (FTIR) spectroscopy quantifies OM by functional groups rather than individual compounds, providing a compromise between bulk OC (such as evolved gas analysis, EGA, or thermal-optical transmittance, TOT, and high-resolution gas chromatography, or HRGC) and speciation techniques (such as gas chromatography mass spectrometry, or GCMS) (*12, 15, 16*). FTIR spectroscopy classifies organic compounds by their chemical functionality, whereas EGA and HRGC measure bulk OC and have only limited information provided by temperatures of volatilization. The advantage over GCMS speciation is that nearly all of the organic carbon can be identified, providing a representative cross-section for calculating OM. This work assesses the variability of OM-to-OC values collected in recent studies in the Caribbean (during the Passing Efficiency of the Low Turbulence Inlet Experiment, or PELTI) and in northeastern Asia (as part of the Aerosol Characterization Experiment – Asia, or ACE-Asia). The results illustrate that FTIR-based measurements avoid the molecular mass assumptions used in bulk OC techniques, improving our ability to measure OM in the atmosphere and quantifying the OM contribution to atmospheric aerosol more accurately than EGA measurements. This work also assesses how accurately we can evaluate aging of organic compounds by photochemical processing from measured OM-to-OC values.

Experimental Section

OM-to-OC Ratios. The chemical structure and many of the physical properties of organic compounds can be described by the number of carbon atoms in their chains and the number of functional groups of which they are composed (*17*). Group contribution methods posit that functional groups in a molecule act independently in order to predict the behavior of monofunctional compounds and their mixtures accurately (*3, 17*). For multifunctional compounds, paired groups can be incorporated to account for interacting functional groups (*3, 18*).

Reducing organic compounds to functional groups and carbon chains provides a systematic approach to characterizing organic mass, as shown in Figure 1. The ratio of OM-to-OC varies with the functional group index (FGI, the ratio of the number of functional groups to the number of carbons in the chain) for different classes of organic compounds. For group contribution methods, aromatic and other unsaturated bonds are counted as functional groups in order to show their effect on OM and solubility. The resulting curves describe the OM-to-OC ratios of straight-chain, monofunctional alkane, alkene, aromatic, alkanal, alkanol, alkanone, alkanoic acid, alkyl sulfate, organosulfide, organonitrate, and amine classes. Branched compound classes fall below these lines, since the branched carbons will lower the values of OM-to-OC ratios. Multifunctional compounds have midrange values of OM-to-OC ratios, lying between the monofunctional classes that are representative of their functional groups: amino acids have OM-to-OC values below the FGI-equivalent acid and above the FGI-equivalent amine (for example, comparing a 2-carbon amino acid such as glycine to a 2-carbon dicarboxylic acid and a 2-carbon diamine). Mixtures of these compound classes can be represented as linear combinations of their components.

While Figure 1 clearly illustrates the well-known dependence of OM-to-OC ratios on the class of organic compounds associated with each different line, the dependence on molecular chain length is sometimes overlooked. Recent ambient measurements have used an OM-to-OC ratio of 1.7,

* Corresponding author phone: (609)258-1144; fax: (609)258-0211; e-mail: lrussell@princeton.edu. Mailing address: A317 Engineering Quadrangle, Princeton University, Princeton, NJ 08544.
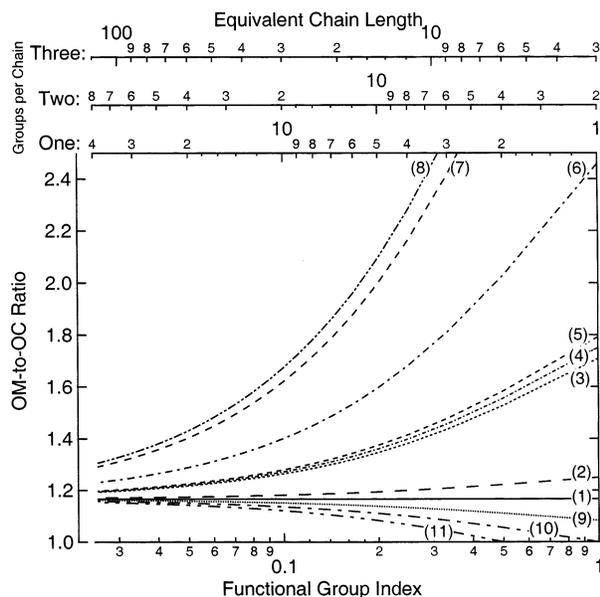
FIGURE 1. Relationship between OM-to-OC ratios and FGI for (1) alkanes, (2) amines, (3) alkanols, (4) alkanones, (5) alkanals, (6) alkanoic acids, (7) alkylnitrates, (8) alkyl sulfates, (9) alkenes or aromatics, (10) branched alkanes, and (11) branched alkenes. Lines are shown connecting discrete points and do not represent continuous functions. Top axes show the equivalent chain length corresponding to one, two, or three groups per chain for the FGI value on the bottom axis.

asserting that the high value results from the increase in oxygenation that occurs with photochemical reactions during processing of emissions in the atmosphere (7, 9). The functional group index for this value would be about 1/4 for an alkanoic acid (or equivalently 2/8 for a diacid), 1/3 for a branched acid, or just under 1/1 for a ketone, meaning that the average chain length given by these small denominators is below 4 carbons for monofunctional compounds and only 8 for straight-chain dicarboxylic acids. While photochemical processes frequently cleave carbon bonds to shorten chains (2), there is little evidence that such short chains dominate organic mass, since they have only been measured to account for less than 5% of organic mass (19). Aromatic polyacids formed from soot or other oxidation processes could account for observations of humic-like substances in atmospheric aerosol (22−24), producing the same OM-to-OC ratio of 1.7 for a large organic molecule consisting of 20 or more repeated acid units of 3 to 4 carbons each.

Calibrated FTIR Spectroscopy. Analysis of aerosol samples by FTIR spectroscopy has been limited by the uncertainties associated with nonuniform sample geometries on impactor substrates and detection limits needed for the preparation of uniform-geometry KBr pellets (25, 26). Particle collection on thin Teflon filters with visibly uniform deposition across the filter allows an in situ analysis without geometric variability in sample deposits. Spectral interference in the Teflon absorption region reduces its accuracy for nearby compounds such as sulfate and other species. In addition, preconcentration of the ambient aerosol minimizes the constraints of instrument detection limits and the required sampling time (27, 28).

OM-to-OC measurements by FTIR spectroscopy detect most of the organic mass that is unresolved in speciated methods such as GCMS and provides some information about the physical and chemical behavior of the functional groups present (polarity, solubility, surface tension). Calibrations to laboratory-generated standards and their mixtures show that the scatter for a mass determination for a single known compound provides a standard deviation of less than 3% for

pure organic standards (28). For an unknown compound with a specific functional group, its absorptivity is taken as the average of the measured standards that contain that functional group. The range of values obtained for different groups giving errors that range from 1% (for aromatic C−H) up to 7% (for C=O). The largest uncertainty of 7% in C=O absorptivities reflects differences for the same functional group in different compounds, for example, from 14.3 for perinaphthenone to 17.4 for adipic acid. Back-filters were collected with each sample and were analyzed by FTIR. Back-filter masses never exceeded detection limits showing no detectable adsorption, but the error in detecting the low loadings of adsorbed mass add an additional uncertainty. The combined uncertainty for FTIR detection, peak integration, and adsorption artifacts are between 5% and 22%, depending on the loading of the back-filter.

Composite OC and OM. The bond absorbance characteristics provided by FTIR characterize a functional group consisting of the bond between a noncarbon atom or heteroatom and a carbon (e.g. C−O) that typically is also bonded to a carbon chain. To quantify OC and OM, the other two (or one) bonds are assumed to be to another carbon and hydrogen (or just two hydrogens). As summarized in Table 1, OM-to-OC ratios for each functional group are used to determine the measured OC and OM as follows

$$OC = 0.5[aC\text{-}H] + [eC\text{-}H] + [rC\text{-}H] + [C\text{-}O] + [C=O] + [C\text{-}N] + [C\text{-}S] \quad (1)$$

and

$$OM = 0.6[aC\text{-}H] + 1.1([eC\text{-}H] + [rC\text{-}H]) + 2.4[C\text{-}O] + 2.3([C=O] + [C\text{-}N]) + 4.5[C\text{-}S] \quad (2)$$

where [aC−H], [eC−H], [rC−H], [C−O], [C=O], [C−N], and [C−S] are the measured moles of bonds of alkane, alkene, aromatic, alcohol, carbonyl, organonitrogen (amine or organonitrate), and organosulfur (organosulfate or organosulfide) (31). OC and OM are calculated in units of g. Note that eqs 1 and 2 do not account for cyclic or branched carbons because tertiary-branched carbons cannot be detected. All other carbon bonds common in the atmosphere are included along with their associated H, O, N, and S masses, with the ratios used for OM-to-OC listed in Table 1.

FTIR Functional Group Errors. Measurements of highly branched compounds will not measure all of the carbon atoms present, causing low OM and OC measurements. Since FGI is overestimated if the number of alkanes is underestimated relative to the number of functional groups, the equivalent chain length (which is interpreted as the number of carbons per functional group) also is underestimated. The algorithms in eqs 1 and 2 used to quantify OC and OM from bonds count a carboxylic carbon twice (one per [C−O] and one per [C=O]), resulting in an overestimate of OM, OC, and chain length. For individual compounds, the estimated OM and OC result in significant errors, as described in Table 1. Comparing the real and FTIR-measured ratios illustrates some of the compound classes for which OC, OM, and OM-to-OC will be inaccurate. For example, carboxylic acids result in double-counting OC, overestimating OM by 27% and underestimating OM-to-OC by 36%.

To estimate an appropriate composite error for the functional-group-based OM-to-OC ratios in ambient measurements, compound-specific errors should be weighted by their abundance in the atmosphere. Variability in organic composition with location, altitude, and time means that this uncertainty is not uniquely determined but rather a preliminary estimate based on current information. While even a single complete speciated inventory of atmospheric

TABLE 1. OM and OC Measurement from FTIR Spectroscopy of Functional Groups[a]

measured bond (functional group)	real OM	real OC	real OM/OC	FTIR OM	FTIR OC	FTIR OM/OC	GCMS sampling study[b]	ΔOM (%)	ΔOC (%)	ΔOM/OC (%)
alkane C—H								6.4	18	13
(CH)H$_2$ (methyl)	15	12	1.25	21	18	1.17	Los Angeles	3.1	4.8	15
(CH)H (alkyl)	14	12	1.17	14	12	1.17	Tokyo (acids only)	2.1	6.8	37
(CH) (alkyl)	13	12	1.08	7	6	1.17	four sources	2.4	3.5	9.5
alkene C—H								1.9	6.5	25
(CH)H (methylene)	14	12	1.17	26	24	1.08	Los Angeles	0.4	0.7	9.6
(CH) (alkene)	13	12	1.08	13	12	1.08	Tokyo (acids only)	6.5	25	71
							four sources	0.6	2.7	120
aromatic C—H								0.8	0.8	3.1
(CH) (aromatic)	13	12	1.08	13	12	1.08	Los Angeles	0.9	1.0	3.9
							four sources	9.0	10	29
branched C—C										
C (only carbon bonds)	12	12	1.00	ND	ND	ND				
carbonyl C=O								2.4	7.6	52
(C=O) (ketonic)	28	12	2.33	28	12	2.33	Los Angeles	1.0	2.0	31
(C=O)OH (carboxylic acid)	45	12	3.75	57	24	2.38	Tokyo (acids only)	5.7	21	110
(C=O)H (aldehyde)	29	12	2.42	35	18	1.94	four sources	0.7	0.7	31
alcohol C—O								2.5	7.8	56
(CO)H (alcohol)	29	12	2.42	29	12	2.42	Los Angeles	1.1	2.0	33
(CO)H=O (carboxylic acid)	45	12	2.38	57	24	2.38	Tokyo (acids only)	6.1	22	110
(CO)C (ether)	40	24	1.67	58	24	2.42	four sources	0.7	0.7	35
amine C—N[c]								3.1	1.7	68
(CN)H$_2$ (amine)	28	12	2.33	28	12	2.33	Los Angeles	4.0	2.4	89
(CN)O$_2$ (organonitrate)	58	12	4.83	58	12	4.83	four sources	1.8	0.5	210
organosulfate C—S[d]								19	33	49
(CS)O$_3$ (organosulfate)	81	12	6.75	55	12	4.54	50:50 mix[d]	19	33	49
(CS)C (organosulfide)	56	24	2.33	109	24	4.54				

[a] "ND" indicates not detected. [b] Rogge et al. (*12*) composite of five-site Los Angeles measurements, identifying approximately 10% of total OM; Kawamura and co-workers (*40, 41*) midpoint value from Tokyo measurements, identifying approximately 2% of total OM measured; Schauer et al. (*13, 32, 33*) midpoint value source sampling, identifying less than 10% of total OM measured. [c] Organonitrates can be distinguished by secondary peaks and were not identified. [d] If neither organosulfate nor organosulfide can be eliminated based on FTIR spectra, then the recommended value is the average 4.54; since no measurements were available the error is estimated from a 50:50 mix of organosulfate and organosulfide, not including carbon chains.

aerosol organic mass does not exist, recent source and field sampling studies provide a good initial estimate. Starting with the compounds identified by GCMS for Los Angeles ambient (*12*) and stack (*13, 32, 33*) sampling, Figure 2(a,b) compares the real values with the measured values for each compound, showing the expected measurement bias for aromatic compounds. For compounds in which cyclic and branched aromatics dominate, the functional group index has a large uncertainty, and FTIR is likely to overestimate the number of functional groups or equivalently to underestimate the chain length. The large error bars for compounds with OM-to-OC < 1.1 and FGI > 0.6 (such as benzo[ghi]perylene, coronene, and benzo[k]fluoranthene in Figure 2(a,b)) are measured by FTIR as having FGI ≈ 1 because 12 of their 24 carbons are multiply branched and are bonded only to other carbons. The extent to which these errors will systematically bias the data depends on whether these compounds with large systematic errors are present in significant amounts. In some cases, overestimates and underestimates are canceled in the complex organic mixtures present in atmospheric particles. Five Los Angeles area ambient samples, for which approximately 10% of the measured organic mass was resolved into approximately 80 compounds, indicate that FTIR spectroscopy will underpredict the composite OM-to-OC by less than 5% and the functional group index by as much as 10%. GCMS measurements from Tokyo (*40, 41*) characterize only the 2−5% of organic mass that they resolved as acids, ketones, and aldehydes to find a much higher error of 40%. The expected error for each bond in Table 1 was calculated as an average of both Los Angeles and Tokyo sites, weighted by the fraction of OM resolved in each sample.

A carboxylic monoacid/diacid mixture (*34*) illustrates a highly oxygenated set of examples, as illustrated in Figure 2(c). OM-to-OC is underpredicted by only 3%, even though three of the four acids in the mixture have errors higher than 10% as pure compounds. FTIR spectroscopy of glutaric acid measures more OM, OC, and functional groups than are present because eq 1 counts the carbons in both acid groups twice, resulting in the OM-to-OC ratio being 16% too low (since the additional carbons are a bigger proportion of the denominator than the numerator). For 3-hydroxy-4-methylbenzoic acid and pinonic acid, the overcounting of OM in eq 2 outweighs the smaller overcounting of OC, making the OM-to-OC ratio 10% high. In palmitic acid, the two effects balance to make the OM-to-OC ratio less than 1% high.

Results

Concentrated aerosol particle samples were collected by aircraft and ship-based sampling aboard the NCAR C130 in St. Croix (in July 2000 PELTI) and near Japan on the same aircraft as well as on the NOAA R/V *Ronald H. Brown* between Hawaii and Japan (both as part of ACE-Asia in March and April 2001) (*28, 31, 35*). The particle samples on stretched Teflon filters were analyzed by transmission FTIR, quantified with laboratory-generated standards for alkane, alkene, aromatic, alcohol, carbonyl, organonitrogen, and organosulfur functional groups. The results in Figure 3 show a large range of OM-to-OC values with variations in altitude, nearby sources, and sampling location, and the frequency distributions illustrate the limitations of describing the OM-to-OC ratio with a mean value.
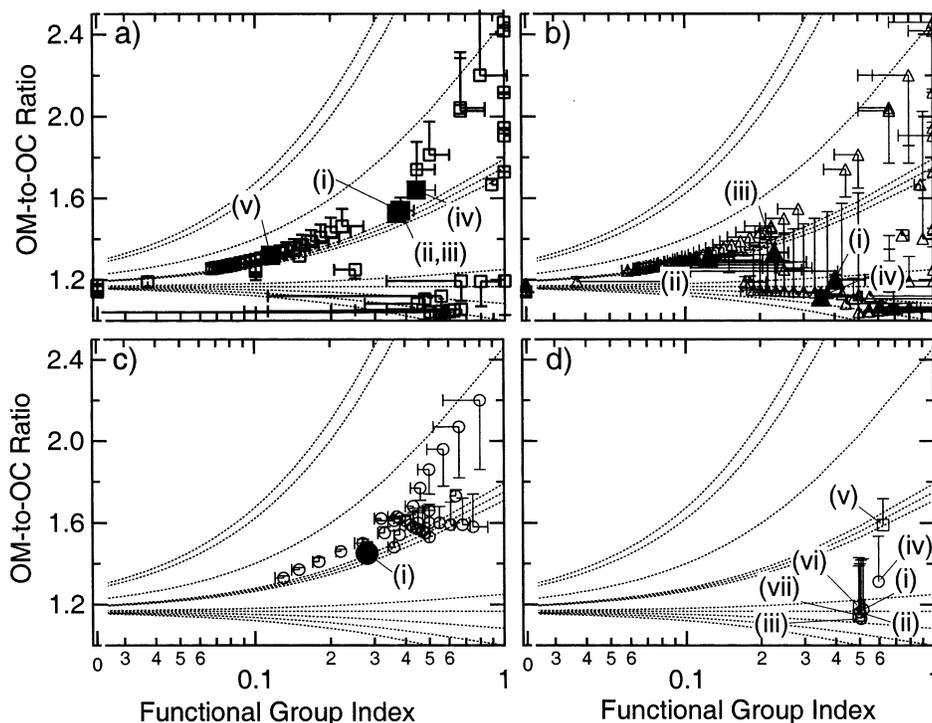
FIGURE 2. OM-to-OC ratio dependence on FGI for organic compounds measured in atmospheric samples and sources. Whiskers indicate the values measured by FTIR for the same compound or mixture; dotted lines show the position of organic class OM-to-OC relationships shown in Figure 1 as guidelines. (a) Compounds (open squares) and mixtures (solid squares) measured at Los Angeles area sites (i) West LA, (ii) Downtown, (iii) Pasadena, (iv) Rubidoux, and (v) San Nicholas Island (12). (b) Compounds (open triangles) and mixtures (solid triangles) measured for sources of (i) diesel engines, (ii) meat charbroiling, and (iii) catalyzed and (iv) noncatalyzed gasoline engines (13, 32, 33). (c) Compounds (open circles) and (i) average monoacid/diacid mixture (solid circle) (34). (d) Samples measured (i) winter, (ii) spring, (iii) summer, and (iv) fall (circles) in northern Italy (39), and separated fractions for (v) neutral compounds, (vi) monoacids and diacids, and (vii) polyfunctional compounds.
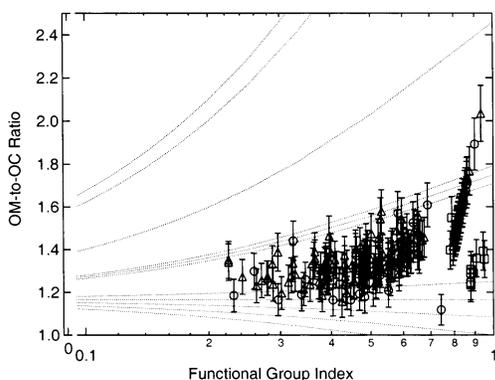

FIGURE 3. OM-to-OC ratio dependence on FGI for submicron aerosol samples measured by FTIR spectroscopy on the NCAR C130 during PELTI (squares), on the C130 during ACE-Asia (triangles), and on the R/V *Ronald H. Brown* during ACE-Asia (circles) (28, 31, 35). Whiskers indicate estimated theoretical errors in the OM-to-OC calculation from functional groups, excluding instrument and sampling errors; dotted lines show the position of organic class OM-to-OC relationships shown in Figure 1 as guidelines.

OM-to-OC Variability. OM-to-OC ratios for all three projects span the range $0 < FGI < 1$ and $1.0 < OM$-to-OC < 2.2. Most of the values lie below the alkanoic acid and above the alkene/aromatic lines shown in Figure 1. All values necessarily fall above the alkene/aromatic lines since no data on cyclic or branched carbons are available. Most values lie in the range $0.3 < FGI < 0.8$ and $1.2 < OM$-to-OC < 1.6. Species measured below detection limit are calculated as half the detection limit where we have omitted values with insufficient mass for characterization of the OM-to-OC ratio.
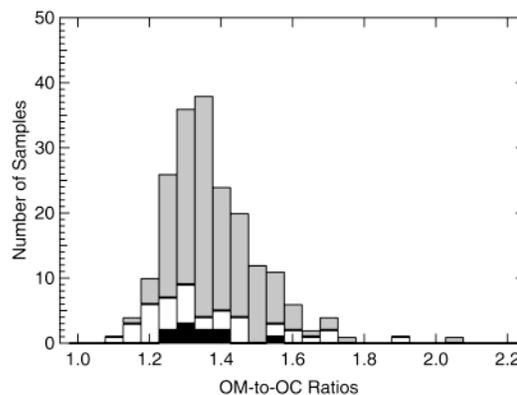

FIGURE 4. Frequency distribution of OM-to-OC ratios for submicron aerosol samples measured by FTIR spectroscopy (i) on the NCAR C130 during PELTI (black), (ii) on the C130 during ACE-Asia (gray), and (iii) on the R/V *Ronald H. Brown* during ACE-Asia (white) (28, 31, 35).

For the Caribbean samples, the average value of OM-to-OC for airborne samples between 30 and 3000 m was 1.34 with a standard deviation of 0.1. Most of the sampled OM-to-OC ratios cluster between 1.2 and 1.4. This means that the typical literature value of 1.4 (36) would have had less than 10% error for 5 of the 10 samples for which OM-to-OC ratios were quantified, as indicated by the PELTI samples in the frequency distribution shown in Figure 4.

In eastern Asia in March and April of 2001, ACE-Asia measurements recorded a project average of 1.38 with a standard deviation of 0.1 for 163 airborne measurements collected aboard the NCAR C130 between 30 and 7000 m. The frequency distribution of OM-to-OC ratios in Figure 4

shows most of the samples between 1.2 and 1.6 with a peak in frequency at 1.4, with 60% of the samples falling within ±10% of the mean. For the R/V *Ronald H. Brown* samples taken approximately 10 m above sea level, the ratio of OM-to-OC averaged 1.36 with a standard deviation of 0.2 for samples of 2−48 h duration. Only 29% of the samples (out of 40 measured ratios) fall within ±10% of the mean. The low values are dominated by alkanes and alkenes with contributions from carbonyls and alcohols. Organosulfur, with its high OM-to-OC ratio of 4.5, accounts for less than 2% of the organic carbon present.

Both surface and airborne measurements in ACE-Asia are skewed toward lower values of OM-to-OC, lying below both the older literature estimate of 1.4 and the urban and nonurban aerosol values (1.6 and 2.1, respectively) (*11, 36*). This lower value is indicative of unsaturated bonds from alkene and aromatic compounds (including polycyclic structures) and indicates that few of the emitted hydrocarbons have been oxygenated during photochemical or other processing in the atmosphere, as addition of oxygen atoms will tend to increase the OM-to-OC ratio. The histograms also clearly show a large variability of ratios from 1.2 to 1.6 with frequent outliers as high as 2.0 within each study region. While this variability is expected given the heterogeneous nature of the PELTI and ACE-Asia regions, it means that the use of a constant value of 1.7 rather than measured OM-to-OC ratios will result in a frequent error of 20% or more. Ten of the 200 ship-based and aircraft-based ACE-Asia samples had OM-to-OC ratios above 1.6, incurring errors of up to 40% if the mean value of 1.4 were used to approximate these samples.

The majority of particles with organic mass above 1 μg m^{-3} have OM-to-OC ratio between 1.2 and 1.6. This observation is consistent with the proposed correlation between more recent emissions with higher mass loadings and lower OM-to-OC ratios as well as with the more aged and processed particles with lower mass loadings due to particle sinks having higher OM-to-OC ratios (*11*).

Discussion

Organic Sampling Errors. If the composition of organic mass is only a weak function of aerosol size, inlet efficiencies, tubing losses, and concentration factors are likely to have small effects on relative concentrations, including OM-to-OC ratios. The assumption that organic composition (and OM-to-OC ratio) is size independent can neither be supported nor contradicted by data due to the shortage of size-resolved organic composition measurements. The variety of primary and secondary organic mass sources suggests that there may be strong signatures of secondary organic compounds in the accumulation mode, while the Aitken nuclei are dominated by combustion-derived primary organic and elemental carbon particles (*2*). Larger particles, at and above 1 μm diameter, may have significant contributions from vegetative detritus (*2*) or other biogenic organic compounds associated with sea salt particles (*3*). The bulk submicron sampling performed here is inadequate for resolving such size-dependent composition differences and can only be addressed with multistaged sampling. The possible size dependence of OM-to-OC and the sampling error in the size specificity of the cutoff diameters of the combined inlet, concentrator, and impactor adds an estimated 15% uncertainty, even though the integrated mass error has been found to be 10% in a limited intercomparison (*31*).

FTIR analysis with collection on prescanned Teflon filters reduces artifacts that interfere in sampling organic compounds in the particle phase (*7, 37*), resulting in the errors summarized in Table 2. The FTIR analysis errors for this technique were typically almost 50% because of the low ambient loadings of PELTI. The ACE-Asia project errors were

TABLE 2. OM Measurement Errors from EGA and FTIR Spectroscopy

	FTIR			EGA[a]		
error	min.	max.	mean	min.	max.	mean
Systematic						
instrument calibration[b]	5%	22%	14%	30%	50%	40%
adsorption on filter	incl.[c]	incl.[c]	incl.[c]	30%	50%	40%
volatilization losses from filter[d]	5%	20%	13%	50%	50%	50%
OM-to-OC ratio[e]	6%	15%	10%	30%	50%	40%
inlet, concentrator, flow rates, size cutoff[f]	5%	15%	10%	15%	20%	18%
Total						
OM total error	11%	35%	24%	NA	NA	
error without inlet	9%	33%	21%	74%	102%	87%
error with 70% error in OM-to-OC ratio	NA	NA	NA	NA	113%	NA

[a] Errors for EGA method are reported by Huebert and Charlson (*7*) and Putaud et al. (*9*). "NA" indicates not applicable. [b] Minimum error is the precision of the calibration for pure standards (*15*) with no uncorrected adsorption artifacts; maximum error was the average instrument error including back-filter quantification errors for the sample loadings collected on the C130 in ACE-Asia (*28*). [c] These errors are included in the instrument calibration errors and are not shown separately. [d] Error is estimated based on undenuded samples, low surface area, short sampling time, and Teflon substrate. [e] Minimum error is the average error for direct OM quantification from functional groups, calculated for the resolved fraction of Los Angeles aerosol (*12*) and Tokyo aerosol (*40, 41*), with each weighted by the fraction of OM identified; maximum error is the average error for OM quantification from the product of OC and OM/OC from functional groups. [f] Minimum error is average PELTI difference between gravimetric and integrated PCASP submicron mass (*15*); maximum accounts for cutoff sizing differences that vary with ambient particle distributions.

25% since the high ACE-Asia filter loadings made Teflon adsorption negligible (*28, 31*). Volatilization losses were not characterized. The samples were undenuded, short, and largely homogeneous so that this artifact is expected to result between 5% and 15% uncertainty. Measurements with polyurethane foam backup capsules are needed to characterize accurately the semivolatile fraction without positive or negative artifacts (*32*).

EGA and FTIR errors are compared in Table 2. The overall errors in the OC calculation by FTIR have also been compared side-by-side to simultaneous evolved gas analysis (EGA) measurements, showing a weak correlation (*31, 38*). The small systematic offset and scatter result from differences in inlets, cutoff concentration diameters, and the inherently different operational OC definitions.

Comparison to Other Estimates. Two other techniques provide information about the OM-to-OC ratio: HNMR with HPLC (*22, 39*) and GCMS (*15, 30*). For comparison, HNMR functional group data were used to estimate OM, OC, and their ratio with assumptions analogous to the ones given in Table 1. Figure 2(d) illustrates this calculation for seasonal measurements from northern Italy (*39*), showing OM-to-OC values between 1.1 and 1.3. The highest value was 1.3 in the fall. The OM-to-OC ratios associated with the neutral and monoacid/diacid fractions had OM-to-OC ratios of 1.2, while the neutral fraction had an OM-to-OC fraction of 1.6. The error estimate in OM-to-OC ratio from HNMR data was more than 20% due to the lack of specificity for the distribution of types of [H−C−C≡] groups quantified (*39*).

The average composition measured for the Los Angeles area (*12*) gives an OM-to-OC ratio of 1.6 for the measured species, which represented 10% of the total organic mass. The FTIR-based estimate for the same sample would be 1.5, or about 5% low, as shown for both the individual species and the mixture in Figure 2(a). The remaining 90% of organic mass could be much more oxygenated or more unsaturated,

so that from only GCMS measurements an appropriate range for the OM-to-OC ratio for this sample would be 1.1 to 2.8, or an uncertainty of about 50%. The particle components and internally mixed compositions for meat charbroiling, diesel engines, and catalyzed and noncatalyzed gasoline engines for the resolved fraction (<5% of measured particulate organic mass) are shown in Figure 2(b), with average OM-to-OC ratios of 1.3, 1.2, 1.3, and 1.1, respectively (*13, 32, 33*). For these compositions, an FTIR-based measurement would underestimate the equivalent chain length and OM-to-OC ratio by 1% to 3%, which is a significant improvement over the GCMS limitation that more than 80% of OM cannot be resolved. Figure 2(c) shows that the average composition of a carboxylic acid mixture (*34*) has a low combined offset of 3%, because the 16% underestimate of 3-hydroxy-4-methyl benzoic acid is canceled by 10% overestimates of glutaric and pinonic acids. In general, for the speciated atmospheric samples studied, the FTIR error in the OM-to-OC ratio was underpredicted by as much as 5%.

Implications for Organic Particle Measurements. Measuring functional groups provides a simplified approach to characterization of organic mass. Its application is limited to characterizing average chemical properties of the mixture rather than identifying individual compounds since mixtures of compounds that have different functional groups and different chain lengths and mixtures of functional groups on individual compounds with one or more functional groups and chain lengths cannot be distinguished. The uncertainty associated with quantifying chemical species by FTIR varies up to 21% (including adsorption but not inlet artifacts) and errors of up to 15% in measuring composite OM-to-OC ratios from functional groups using actual atmospheric mixtures, for a combined error of ca. 26%. OM calculated directly from FTIR has a reduced combined error of only 9% because the higher error in OC quantification is avoided.

Quantifying OM-to-OC ratio is a significant improvement over an estimated uncertainty of ±50% for EGA measurements of OM from uncorrected quartz filter sampling (*7*). While the implied range from this uncertainty of 0.9–2.5 encompasses all measured values, few values were within ±15% of the 1.7 mean used in other studies (*9*) for all three data sets. Employing an OM-to-OC value of 1.7 for the samples shown here would mean that OM is systematically overestimated more than 90% of the time. The improvement is also clear for FTIR-measured samples with OM-to-OC values of 2.0 ± 0.2, for which OM would be underestimated by 43% for the more widely used EGA correction of 1.4. Functional groups provide an estimate of organic mass, with errors less than 25% for measured complex mixtures of organic compounds. Table 2 shows that FTIR spectroscopic analysis of organic carbon groups improves current organic measurements by reducing the maximum error from 102% to 33% or alternatively by reducing the minimum error from 74% to 9%. Smaller uncertainties in organic measurements will greatly improve our assessment of key climate and air quality issues (*7, 9*).

Literature Cited

(1) Novakov, T.; Penner, J. E. *Nature* **1993**, *365*, 823–826.

(2) Seinfeld, J. H.; Pandis, S. N. *Atmospheric Chemistry and Physics*; John Wiley & Sons: New York, 1998.

(3) Ming, Y.; Russell, L. M. *J. Geophys. Res.* **2001**, *106*, 28259–28274.

(4) Adams, P. J.; Seinfeld, J. H.; Koch, D.; Mickley, L.; Jacob, D. *J. Geophys. Res.* **2001**, *106*, 1097–1111.

(5) Stober, W.; Mauderly, J. L. *Inhal. Toxicol.* **1994**, *6*, 427–457.

(6) Iwai, K.; Adachi, S.; Takahashi, M.; Moller, L.; Udagawa, T.; Mizuno, S.; Sugawara, I. *Environ. Res.* **2000**, *84*, 255–264.

(7) Huebert, B. J.; Charlson, R. J. *Tellus* **2000**, *32B*, 1249–1255.

(8) Saxena, P.; Hildemann, L. M. *J. Atmos. Chem.* **1996**, *24*, 57–109.

(9) Putaud, J.-P.; Van Dingenen, R.; Mangoni, M.; Virkkula, A.; Raes, F.; Maring, H.; Prospero, J. M.; Swietlicki, E.; Berg, O. H.; Hillamo, R.; Mäkela, T. *Tellus* **2000**, *52B*, 141–168.

(10) Turpin, B. J.; Saxena, P.; Andrews, E. *Atmos. Environ.* **2000**, *34*, 2983–3013.

(11) Turpin, B. J.; Lim, H.-J. *Aerosol Sci. Technol.* **2001**, *35*, 602–610.

(12) Rogge, W. F.; Mazurek, M. A.; Hildemann, L. M.; Cass, G. R.; Simoneit, B. R. T. *Atmos. Environ.* **1993**, *27A*, 1309–1330.

(13) Schauer, J. J.; Kleeman, M. J.; Cass, G. R.; Simoneit, B. R. T. *Environ. Sci. Technol.* **2002**, *36*, 1169–1180.

(14) Yu, J. Z.; Flagan, R. C.; Seinfeld, J. H. *Environ. Sci. Technol.* **1998**, *32*, 2357–2370.

(15) Hildemann, L. M.; Mazurek, M. A.; Cass, G. R.; Simoneit, B. R. T. *Aerosol Sci. Technol.* **1994**, *20*, 303–317.

(16) Duce, R. A.; Mohnen, V. A.; Zimmerman, P. R.; Grosjean, D.; Cautreels, W.; Chatfield, R.; Jaenicke, R.; Ogren, J. A.; Pellizari, E. D.; Wallace, G. T. *Rev. Geophys. Space Phys.* **1983**, *21*, 921–952.

(17) Fredenslund, A.; Jones, R. L.; Prausnitz, J. M. *AIChE J.* **1975**, *21*, 1086–1091.

(18) Ming, Y.; Russell, L. M. *AIChE J.* **2002**, *48*, 1330–1347.

(19) Kawamura, K.; Kasukabe, H.; Barrie, L. *Atmos Environ.* **1996**, *30*, 1709–1722.

(20) Kawamura, K.; Sempere, R. *Atmos. Environ.* **1994**, *28*, 449–459.

(21) Kawamura, K.; Ikushima, K. *Environ. Sci. Technol.* **1993**, *27*, 2227–2235.

(22) Decesari, S.; Faccini, M. C.; Fuzzi, S.; Tagliavini, E. *J. Geophys. Res.* **2000**, *105*, 1481–1489.

(23) Facchini, M. C.; Fuzzi, S.; Zappoli, S.; Andracchio, A.; Gelencsér, A.; Kiss, G.; Krivácsy, Z.; Mészáros, E.; Hansson, H.-C.; Alsberg, T.; Zebühr, Y. *J. Geophys. Res.* **1999**, *104*, 26821–26832.

(24) Krivácsy, Z.; Kiss, G.; Varga, B.; Galambos, I.; Sarvari, Z.; Gelencsér, A.; Molnar, A.; Fuzzi, S.; Facchini, M. C.; Zappoli, S.; Andracchio, A.; Alsberg, T.; Hansson, H. C.; Persson, L. *Atmos. Environ.* **2000**, *34*, 4273–4281.

(25) Blando, J. D.; Porcja, R. J.; Turpin, B. J. *Aerosol Sci. Technol.* **2001**, *35*, 899–908.

(26) Allen, D. T.; Palen, E. J.; Haimov, M. I.; Hering, S. V.; Young, J. R. *Aerosol Sci. Technol.* **1994**, *21*, 325–342.

(27) Sioutas, C.; Koutrakis, P.; Burton, R. M. 1994. *J. Aerosol Sci.* **1994**, *25*, 1321–1330.

(28) Maria, S. F.; Russell, L. M.; Turpin, B. J.; Porcja, R. J. *Atmos. Environ.* **2002**, *36*, 5185–5196.

(29) Hildemann, L. M.; Mazurek, M. A.; Cass, G. R.; Simoneit, B. R. T. *Environ. Sci. Technol.* **1991**, *25*, 1311–1325.

(30) Kawamura, K.; Gagosian, R. B. *J. Chromatogr.* **1988**, *438*, 299–307.

(31) Maria, S. F.; Russell, L. M.; Turpin, B. J.; Porcja, R. J.; Campos, T. L.; Weber, R. J.; Huebert, B. J. *J. Geophys. Res.* **2003**, submitted.

(32) Schauer, J. J.; Kleeman, M. J.; Cass, G. R.; Simoneit, B. R. T. *Environ. Sci. Technol.* **1999**, *33*, 1578–1587.

(33) Schauer, J. J.; Kleeman, M. J.; Cass, G. R.; Simoneit, B. R. T. *Environ. Sci. Technol.* **1999**, *33*, 1566–1577.

(34) Hemming, B. L.; Seinfeld, J. H. *Ind. Eng. Chem. Res.* **2001**, *40*, 4162–4171.

(35) Rivera, M. D. Master's Thesis, Princeton University 2003.

(36) White, W. H.; Roberts, P. T. *Atmos. Environ.* **1977**, *11*, 803–812.

(37) Mader, B. T.; Pankow, J. F. *Environ. Sci. Technol.* **2001**, *35*, 3422–3432.

(38) Bertram, T.; Huebert, B. J.; Howell, S.; Blomquist, B.; Heath, J. *J. Geophys. Res.* **2003**, manuscript in preparation.

(39) Decesari, S.; Faccini, M. C.; Matta, E.; Lettini, F.; Mircea, M.; Fuzzi, S.; Tagliavini, E.; Putaud, J.-P. *Atmos. Environ.* **2001**, *35*, 3691–3699.

(40) Kawamura, K.; Ikushima, K. *Environ. Sci. Technol.* **1993**, *27*, 2227–2235.

(41) Sempere, R.; Kawamura, K. *Atmos. Environ.* **1994**, *28*, 449–459.